HHS Public Access

Author manuscript

Anal Chem. Author manuscript; available in PMC 2020 April 02.

Published in final edited form as:

Anal Chem. 2019 April 02; 91(7): 4618–4624. doi:10.1021/acs.analchem.8b05885.

Cavity Carbon Nanopipette Electrodes for Dopamine Detection

Cheng Yang[1], **Keke Hu**[2,3], **Dengchao Wang**[2], **Yasmine Zubi**[1], **Scott T. Lee**[1], **Pumidech Puthongkham**[1], **Michael V. Mirkin**[2,3], and **B. Jill Venton**[1,*]

[1]Department of Chemistry, University of Virginia, Charlottesville, VA 22904

[2]Department of Chemistry and Biochemistry, Queens College–CUNY, Flushing, New York 11367

[3]The Graduate Center of the City University of New York, New York, New York 10016

Abstract

Microelectrodes are typically used for neurotransmitter detection, but nanoelectrodes are not because there is a trade-off between spatial resolution and sensitivity, which is dependent on surface area. Cavity carbon nanopipette electrodes (CNPEs), with tip diameters of a few hundred nanometers, have been developed for nano-scale electrochemistry. Here, we characterize the electrochemical performance of CNPEs with fast-scan cyclic voltammetry (FSCV) for the first time. Dopamine detection is compared at cavity CNPEs, with a depth equivalent to a few radii, and open-tube CNPEs, an essentially infinite geometry. Open-tube CNPEs have very slow temporal response that changes over time as the liquid rises in the pipette. However, the cavity CNPEs have a fast temporal response to a bolus of dopamine that is not different than traditional carbon-fiber microelectrodes. Cavity CNPEs, with a tip diameter of 200-400 nm, have high currents because the small cavity traps and increases the local dopamine concentration. The trapping also leads to a FSCV frequency independent response and the appearance of cyclization peaks that are normally observed only with large concentrations of dopamine. CNPEs have high dopamine selectivity over ascorbic acid (AA) due to the repulsion of AA by the negative electric field at the holding potential and the irreversible redox reaction. In mouse brain slices, cavity CNPEs detected exogenously-applied dopamine, showing they do not clog in tissue. Thus, cavity CNPEs are promising neurochemical sensors that provide spatial resolution on the scale of hundreds of nanometers, useful for small model organisms or locating near specific cells.

Graphical Abstract

*Corresponding author: jventon@virginia.edu, Phone 434-243-2132.

Supporting Information

The supporting information contains 3 figures, S1: FSCV response to 1 μM dopamine at an open tube CNPE, S2: numerical simulations of double layer and preconcentration in the CNPE tip, and S3: comparisons of simulations of response at a conical nanofiber and cavity nanopipette. Supplemental methods are also provided for the finite element simulation of CNPEs for dopamine detection

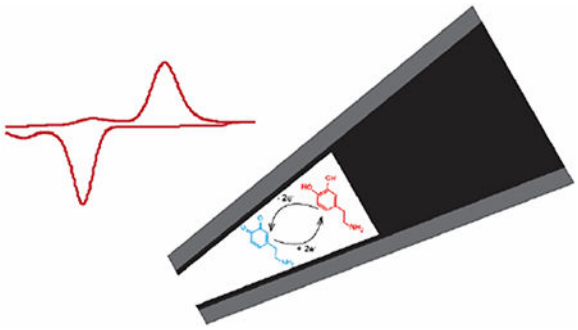

Neurochemical detection *in vivo* has predominantly been performed with microelectrodes. Carbon-fiber microelectrodes (CFMEs), with a diameter of 7 μm and length of 50 - 100 μm, are the most popular electrodes for direct detection of electroactive species. While these electrodes work well for measuring average changes in rodent brains, there are a variety of other applications that would benefit from robust and sensitive nanoelectrodes. Small animal models such as *Drosophila* and zebrafish are easy to genetically manipulate,[1–3] but the small dimensions of their central nervous systems require better spatial resolution to implant the probe into a specific brain region.[4–7] In addition, measurements of neurotransmitters are being made in single synapses, which require an electrode with a nanosized tip, preferably in a disk geometry.[8] Carbon nanofiber microelectrodes fabricated on large silicon chips have been developed for neurotransmitter detection, but the large dimensions of the chip and the geometry limit the implantation.[9] Flame-etching or electrochemically-etching carbon fibers can create finite conical nanoelectrodes with 50–200 nm tip diameters, but they are still micron scale in length.[8,10] Etching requires nanoelectrodes to be fabricated individually and reproducibility is poor. Robust, sensitive, and easy to fabricate nanoelectrodes would enable many new types of experiments and play a crucial role in understanding neurotransmission and neuromodulation.[11]

Nanometer-scale pipettes pulled from borosilicate or quartz capillary have been widely used in bio-analysis[12], nanoelectrochemistry[11], and scanning probe microscopies[13,14]. Nanoscale carbon pipette electrodes are also useful for localized detection of neurotransmitters at the level of single cells, single vesicles, as well as single synapses.[8,9,11,15–17] For nanopipette electrodes, carbon is selectively deposited on the inner wall of a pulled capillary by chemical vapor deposition (CVD) with controllable thickness of carbon film. The process facilitates batch fabrication with high reproducibility. Takahashi et al. described the pyrolytic decomposition of carbon precursor gases inside pulled quartz glass nanopipettes which produces nanometer carbon electrodes with small overall dimensions at the probe tip.[18] Carbon nanopipettes have been successfully utilized for injection of chemicals into living cells,[19] as ohmic nanoelectrodes for intracellular electrophysiological recording of responses to pharmacological agents,[20] and as nanoelectrodes for the measurement of reactive oxygen and nitrogen species in cells.[21] Our group has reported the application of small, robust, and sensitive closed-tip conical carbon nanopipettes (CNPEs) for the *in vivo* detection of endogenous dopamine release in *Drosophila* larvae.[15] While the tip diameter is submicron, the length is on the scale of tens of microns, controlled by etching the quartz away. Since the electrochemical signal is proportional to the surface area of the electrodes, the balance

between sensitivity (larger surface area) and spatial resolution (smaller detection dimension) is always difficult and nanoelectrodes have had limited application in tissue.

The goal of this study was to characterize CNPEs that truly sample from a nanometer sized region for detection of neurotransmitters. CNPEs were made with either a cavity (i.e., the depth is equivalent to a few pipette radii, also known as nanosamplers[16]) or open tube (essentially infinite) geometry. The electrodes thus only sample at the tip and the spatial resolution is equivalent to the diameter of the tip. However, the cavity or open tube geometry provides a large active carbon surface area inside the nanoelectrodes. We characterized CNPEs with open tubes and cavity geometries with fast scan cyclic voltammetry (FSCV)[4,22] for the first time, and found that cavity CNPEs have sufficient temporal resolution and sensitivity for dopamine. The small cavity traps and increases the local dopamine concentration, which improves currents, but the trapping does not slow the temporal response, which is on the order of seconds. High selectivity is observed for dopamine detection over ascorbic acid because of the enhanced electric field and the redox cycling for dopamine. Thus, cavity CNPEs are true nanoelectrodes that can provide spatial resolution in the hundreds of nanometers range, while still maintaining enough current to detect physiological levels of neurotransmitters.

Experimental Section

Electrochemistry

FSCV was performed with a ChemClamp potentiostat (Dagan, Minneapolis, MN, with 1 MOhm Headstage). The waveform was generated, and the data was collected using a High Definition Cyclic Voltammetry (HDCV) breakout box, HDCV analysis software program (UNC Chemistry Department, Electronics Design Facility) and PCIe-6363 computer interface cards (National Instruments, Austin, TX). Electrodes were backfilled with 1 M KCl and a silver wire was inserted to connect the electrode to the potentiostat headstage. The typical triangular waveform swept the applied potential from −0.4 V to 1.3 V at 400 V/s versus an Ag/AgCl reference electrode, at a scan repetition frequency of 10 Hz. The repetition rate was varied for some experiments.

Electrodes were tested using a flow-injection system, as previously described.[23] Analyte was injected for 5 seconds and current versus time traces were obtained by integrating the current in a 100 mV window centered at the oxidation peak for each cyclic voltammogram (CV). Background-subtracted CVs were calculated by subtracting the average of 10 background scans, taken before the compound was injected, from the average of five CVs recorded after the analyte bolus was injected.

Carbon Nanopipette Electrode Fabrication

Nanopipettes were heat-pulled from quartz capillaries (1.0mm outer diameter and 0.5/0.7 inner diameter, Sutter Instrument, Novato, CA) and their inside was coated with carbon by chemical vapor deposition (CVD) to yield open tube or cavity CNPEs. Specifically, nanopipettes with tip diameters of 200-400 nm were pulled using pulling programs based on HEAT=650, FIL=3, VEL= 22, DEL=135, PULL=85. Cavity CNPEs were fabricated by 1

hour CVD with methane and argon (1:1 ratio) at 945°C, while an open tube CNPE was fabricated by 45 min CVD with methane and argon (5:3 ratio) at 950°C. All the parameters were adjusted slightly to obtain required size and geometry.

Surface Characterization

A JEOL JEM-2100 transmission electron microscope (TEM) was used to characterize the carbon distribution near the tip of the nanopipette. The pipette was attached to the grid (PELCO Hole Grids, Copper) in such a way that its tip was shown in the grid center hole, and the rest of the pipette was cut off. A relatively low electron beam voltage of 120 kV was used to reduce charge/heat accumulating effects on the glass layer.

Finite Element Simulation

The finite element simulation of the cavity carbon nanopipettes electrodes for dopamine detection was conducted using COMSOL Multiphysics 5.3a, and a detailed description of the simulation is in the Supporting Information. Briefly, following the earlier report,[15] a 2D axisymmetric model was built to model the voltammogram of the dopamine. The “Transport of Dilute Species” and “Electrostatics” modules are coupled to simulate the electrochemical processes, and the electric double layer structure at the carbon/solution interface. A time dependent solver was used to simulate the cyclic voltammogram at high potential scan rate of 400 V/s.

Brain Slice Experiments

Exogenous application of dopamine in mouse brain slices was used to test the CNPE’s performance in tissue. All animal experiments were approved by the Animal Care and Use Committee of the University of Virginia. C57BL/6 mice (6-8 weeks, Jackson Labs) were housed in a vivarium and fed and given water *ab libitum.* The mice were anesthetized with isoflurane, sacrificed using cervical dislocation, and beheaded immediately. The brain was removed within 2 minutes and placed in chilled (0-5°C) aCSF for 2 minutes. 400 μm sagittal slices of the caudate putamen were prepared using a vibratome (LeicaVT 1000S, Bannockburn, IL), and transferred to oxygenated aCSF (95% O_2 and 5% CO_2) for 1 hour prior to experimentation in order to reach equilibrium. The CNPE was inserted 75 μm into the caudate putamen. The picospritzing micropipettes were made by pulling a 1.2 mm × 0.68 mm glass capillary (A-M Systems, Carlsburg, WA) using a vertical pipette puller (Narishige, Japan). The tip of the pipette was then trimmed to make an opening and marked in order to better visualize it in the tissue. 150 μM of dopamine was pressure ejected into brain slices using a Parker Hannifin picospritzer (Picospritzer III, Cleveland, OH). The picospritzing micropipette was placed 20-30 μm from the CNPE. The picospritzing parameters were 20 psi for 0.02-1.50 seconds which resulted in 5-268 nL of 150 μM dopamine (0.8-40 pmol) being delivered into the tissue. The pipette was calibrated by ejecting dopamine solution into oil and measuring the diameter of the droplet; the volume of the spherical droplet was then calculated ($4/3*\pi*r^3$) and the mols released from the pipette was determined.

Statistics

All values are given as mean ± standard error of the mean (SEM) for n number of electrodes and all error bars are SEM. Paired or unpaired t tests were performed to compare properties between two groups. A one-way ANOVA with Bonferonni post-tests was used to compare effects among multiple groups. All statistics were performed in GraphPad Prism6 (GraphPad Software,Inc., La Jolla, CA).

Results and Discussion

Physical Characterization

Deposition of carbon inside quartz nanopipettes has been extensively studied and deposition conditions optimized to produce different geometries with continuous inner carbon.[16,18,20,24–26] Figure 1 shows TEM images of pipettes with the carbon coated inner wall. The fabricated CNPE geometry is generally described by the aspect ratio $H = h/a$, where h is the depth of carbon-coated cavity and a is the orifice diameter. Tip diameters were 200-400 nm, and while it is hard to precisely determine the depth of the cavity from TEM, due to glass thickness (Fig. 1A), previous estimates with thinner glass show H=12-30.[16] In comparison, open tube CNPEs have a similar tip diameter (~200 nm) but with an open channel in the middle, so the effective aspect ratio is larger than 1000 (Fig. 1B). Because the inside area of the CNPE is coated with carbon, there is a high surface area to volume ratio compared to a disk electrode of similar diameter.

Cavity and Open-tube CNPEs Comparison

The response of CNPEs was tested with FSCV using a typical dopamine waveform of −0.4 to 1.3 V and back at 400 V/s and a scan repetition frequency of 10 Hz. Figure 2 shows examples of background charging current CVs, background-subtracted CV for 5 μM dopamine, and the oxidation current vs time response to a bolus of dopamine. Electrodes were equilibrated by applying the waveform in solution for 30 min. The electrodes are very small, as evidenced by the small background charging currents which are on the order of 10 nA, not hundreds of nA seen for CFMEs.[4] The CVs have oxidation and reduction peaks that are nearly symmetrical in current, indicating a much better reversibility than traditional CFMEs. The ΔE_p for dopamine is 0.7 V for both cavity and open tube but the peaks are slightly shifted (~0.2 V) to positive potentials. The CVs also have an extra peak at 0.16 V, due to dopamine cyclization reactions. Scheme 1 shows the oxidation pathway: following the two-electron oxidation of dopamine (a, DA) to dopamine-o-quinone (b, DOQ), ring closure via deprotonation of the amine side chain to leucodopaminechrome (c, LDAC) occurs irreversibly. LDAC is then oxidized to dopaminechrome (d, DAC). The extra peak at 0.16 V is due to the oxidation of LDAC to DAC and is not typically observed at CFMEs at low concentrations. However, cyclization reactions have been observed at long-length CNTs, which can trap the produced species.[27] Here, the CNPE traps the DOQ and increases its local concentration in the cavity, which also amplifies the second redox reaction.

The temporal resolution is key for application of CNPEs using FSCV. The rise time of the cavity CNPE to a bolus injection of dopamine is not different than a CFME ($t_{10\text{-}90\%}$ =1.5 ± 0.1 s CNPE vs 1.2 ± 0.1 s CFME, unpaired t-test, p = 0.2454, n = 5) so these electrodes

are feasible for rapid measurements using FSCV. The rise time for the open tube electrode is much longer ($t_{10\text{-}90\%}$ = 7 s in Fig. 2F, unpaired t-test, $p < 0.0001$), due to the limited mass transfer in “infinitely long” shaft. In fact, the open tube pipette never reaches equilibrium; the signal increases with time as solution continues to wick into the pipette (Fig. S1 shows i vs t curves taken every 5 min). Past studies have shown a recessed tip with large depth-to-orifice ratio leads to a slow temporal response when using FSCV because the analyte gets trapped.[28,29] While back pressure can be applied to the electrode to limit the solution front, this is experimentally challenging and not practical for in vivo measurements. Thus, we chose to proceed with the cavity electrodes instead, which have a controlled size, shorter equilibration time, and faster temporal response.

Electrochemical Characterization of Cavity CNPEs

The electrochemical characteristics of the cavity CNPEs were compared to traditional CFMEs and conical CNPEs tested previously (Table 1).[15] Conical CNPEs have 200-400 radius nm tips with 150 μm lengths, while CFMEs were 7 μm radius tips with 100 μm lengths. Both the dopamine oxidation current and the background charging current are significantly smaller at cavity CNPEs than the other electrodes because the surface area is much smaller (unpaired t-test, $p \leq 0.0001$ for both comparisons). A measure of signal per unit area is the oxidation current to background current ratio, with a larger ratio being better. Cavity CNPEs have a significantly larger ratio than conical CNPEs (unpaired t-test, $p \leq 0.001$) but a smaller ratio than CFMEs (unpaired t-test, $p \leq 0.0001$). The carbon structure of CNPEs is more graphitic and has less surface defects or oxide groups than CFMEs,[30,31] so the CNPEs likely adsorb less dopamine and have lower oxidation current to background current ratios than the CFMEs.

The limit of detection (LOD) for dopamine at the cavity CNPEs (56 ± 13 nM) is larger than those at the conical CNPEs (25 ± 5 nM, unpaired t-test, $p \leq 0.05$) and CFMEs (19 ± 4 nM, unpaired t-test, $p \leq 0.01$). The LOD at cavity CNPEs is likely to be limited by the system noise. The amplifier and filters on the FSCV system are not designed for pA signal detection and thus the noise is proportionally higher for the small electrodes. Electronics could be optimized in the future.

The difference between the oxidative and reductive peak potentials (ΔE_p) at cavity CNPEs falls between the other two electrodes: smaller than CFMEs (unpaired t-test, $p \leq 0.01$) and larger than conical CNPEs (unpaired t-test, $p \leq 0.05$). At CNPEs, the deposited carbon is amorphous with the oxygen-containing functional groups of ~ −0.01 C/m^2.[32] The larger ΔE_p at the cavity CNPEs compared to the conical CNPEs might be due to their different geometry: the mass transport distance would be longer at cavity CNPEs because dopamine needs to diffuse into the cavity; thus, ΔE_p would be larger based on the theory of charge transfer at partially blocked surfaces.[33] In addition, the higher impedance at the cavity CNPEs could increase the ΔE_p.

The CVs show dopamine redox peak potentials that are shifted positively at cavity CNPEs compared to CFMEs (Fig. 2A). The average dopamine oxidation peak potential ($E_{p,a}$) and reduction peak potential ($E_{p,c}$) at cavity CNPEs are 0.73 ± 0.03 V (n = 6) and 0.09 ± 0.02 V (n = 6), respectively, about 200 mV shifted from CFMEs ($E_{p,a}$ 0.49 ± 0.01 V, $E_{p,c}$ −0.17

± 0.01 V, n = 6, unpaired t-test, $p \leq 0.0001$ for both comparisons). The potential shift in the oxidation/reduction peaks is due to the excess surface charges at the carbon layer, originating from the deprotonation of surface functional groups. Modeling of the double layer at the carbon nanopipette surface in Fig. S2 shows the open circuit diffuse layer potential of −15 mV. While that is not as large as the observed shifts, it predicts that the surface does have a negative charge. Potential shifts have also been observed at materials with high amounts of oxygen-containing functional groups,[28,34] and the cavity geometry of the negatively charged carbon in CNPEs could lead to a more predominant effect. In this case, extra voltage needs to be applied for dopamine redox.[2,28]

Detection of Dopamine at Cavity CNPEs and Numerical simulation

CNPEs have enhanced dopamine currents and better reversibility because the negative charge of the surface preconcentrates dopamine and the small cavity traps dopamine, acting like a thin-layer electrochemical cell. Modeling shows the DA concentration near the carbon surface could be 1.5 times higher than its bulk value due to electrostatic interactions and adsorption (Fig. S2C). Therefore, higher than expected currents are obtained with CNPEs for the dopamine detection, because more dopamine is trapped. The CNPEs are also more reversible, as oxidation/reduction currents ratio ($i_{p,a}/i_{p,c}$) at cavity CNPEs are significantly smaller than CFMEs (Table 1, unpaired t-test, $p \leq 0.0001$). In our previous work, we demonstrated that a rough surface with a crevice depth > 1900 nm traps redox molecules, amplifies the signals, and makes them more reversible.[28,29] From numerical simulations, cavity CNPEs have a larger current than that for a conical CNPEs because of the redox cycling (Fig. S3).

Numerical simulations were used to understand the redox processes and concentration of dopamine in the pipette during FSCV. Fig. 3 shows the waveform, with points marked at several potentials. A simulated CV is also shown, with the points also marked. Although the real experimental geometry and electron transfer processes are likely much more complicated (i.e. porous carbon structure, unknown surface charge density, adsorption controlled and functional group dependent), we still observe similar oxidation/reduction peaks in the simulated voltammogram. The bottom of Fig. 3 shows simulations at each voltage of the concentration of dopamine in the pipette. When dopamine is oxidized starting at 0.3 V, the concentration at the carbon surface decreases. At 1.3 V, all the dopamine is depleted in the pipette. At 0.3 V on the anodic scan, dopamine is being reformed as dopamine-o-quinone is reduced back to dopamine. When the potential hits −0.4 V at the end of the scan, all of the dopamine-o-quinone has been regenerated to dopamine, making the cavity concentration the bulk dopamine concertation. Thus, in a cavity CNPE dopamine is rapidly oxidized but rapidly redox recycled during an FSCV scan. These simulations are for a cavity electrode but note that the surface potential and DA concentration profile near the tip region would be the same for the cavity and open-tube CNPEs.

The cavity geometry enhances the electric field at the tip, which enables a stronger electrostatic attraction for positively charged dopamine during the holding potential. One piece of experimental evidence supporting the fact that the electric field is enhanced is that the signal at cavity CNPEs is not dependent on the switching potential. For CFMEs, Fig. 4A

shows that oxidative current is higher after a switching potential of 1.3 V, which is sufficient to break carbon bonds and renew the surface.[35] In contrast, oxidative current does not change for cavity CNPEs with switching potentials of 1.0 to 1.6 V (one-way ANOVA, Bonferroni post-test, $p = 0.2906$). The enhanced electric fields at the tip causes oxidation of carbon even at lower potentials, so there is no effect of switching potential.

The trapping effect at the nanocavity creates thin-layer cell like conditions that lead to other properties, such as a FSCV waveform frequency independent response. Figure 4B shows dopamine oxidation current with scan repetition frequencies from 10 to 100 Hz and current does not significantly change with increasing scan frequency (one-way ANOVA, Bartlett's test, $p = 0.4542$). In comparison, the oxidation current drop is dramatic at CFMEs, with approximately 50% signal loss at 50 Hz and 67% loss at 100 Hz compared to 10 Hz. In addition, the rise time ($t_{10\text{-}90}$) is not different at different scanning frequencies ($t_{10\text{-}90}$ =1.5 ± 0.1 s at 10 Hz vs 1.7± 0.2 s at 100 Hz, paired t-test, $p = 0.4432$, $n = 3$). The frequency independent property enables highly sensitive neurotransmitter detection at rapid repetition frequencies.

Stability and Selectivity Tests

Electrodes are typically used *in vivo* for hours at a time to measure neurotransmission and typical experiments in *Drosophila* are up to two hours long.[36] Figure 4C shows the dopamine oxidation signal is constant for 2 hours of continuous scanning at CNPEs (one-way ANOVA, Bartlett's test, $p > 0.05$, $n = 3$), the same as the traditional CFMEs. Given the enhanced electric fields that may break carbon bonds, it is very promising that these electrodes are stable for 2 hours (1200 FSCV scans).

Ascorbic acid (AA) is a common anionic interferent in extracellular fluid and the selectivity of cavity CNPEs for dopamine over AA was tested.[37–39] Figure 5A shows the CV for 200 μM AA and 1 μM DA and the peak for AA is much smaller than dopamine, even though it is at a higher concentration. The ascorbic acid to dopamine oxidation current ratio is 0.6 ± 0.1 ($n = 5$) at cavity CNPEs, which is significantly lower than at CFMEs (14.6 ± 0.4, $n = 5$, t-test, $p \leq 0.0001$), indicating dramatically improved dopamine selectivity over ascorbic acid at cavity CNPEs (Figure 5B). Previously, different nanomaterials, polymers, surface modifications, and electrochemical techniques have been used to improve the selectivity.[34,40–42] Here, the cavity geometry and the resulting enhanced electric field at the tip pre-concentrates dopamine (Figure S1) and repels negatively charged species such as ascorbic acid. In addition, ascorbic acid has no obvious reduction,[43] indicating an irreversible reaction at the cavity CNPEs, which is different than the reversible reaction at CFMEs.[34,41,44] Thus, there would be no redox cycling for ascorbic acid as there is with dopamine. The promising dopamine selectivity over ascorbic acid is due to both the repulsion by the negative electric field and the irreversible redox reaction.

Measurements of Dopamine in Mouse Brain Slices

To test the stability and robustness for tissue measurements, the cavity CNPEs were tested in mouse brain slices where dopamine was exogenously applied to the tissue. Since the cavity CNPEs are open to their environment, there was a concern that they could be clogged with

tissue. Figure 6A shows that the CNPE is able to detect dopamine in tissue, with different currents for different amounts of dopamine applied; both the primary oxidation and reduction peaks are present in the background subtracted CVs. The ΔE_p increased compared to values obtained from the flow-injection system (Table 1). This increase is a known phenomenon in tissue measurements, likely due to the adsorption of biomolecules to the electrode, which subsequently impedes electron transfer.[52,53] In Figure 6B, the oxidative current versus time plot shows that the dopamine signal decreases after the ejection, demonstrating that the analyte is able to exit the cavity. These results indicate that the cavities of the CNPEs are not being clogged when inserted into tissue, and that they are able to detect the presence of dopamine in tissue.

Conclusions

Cavity carbon nanopipettes are useful nanoelectrodes for detection of dopamine with submicron spatial resolution. There are two main effects that lead to desirable electrochemical properties: analyte trapping and an enhanced electric field. First, the small cavity of CNPEs traps dopamine, allowing exhaustive redox cycling, and leading to high sensitivity since the DA concentrations are much higher than the bulk value. The trapping effect also leads to the appearance of secondary peaks due to cyclization of oxidation products and a FSCV frequency independent response. Second, the enhanced electric field at the tip gives rise to an enhanced selectivity over ascorbic acid and a response that is independent of the switching potential. CNPEs can be used in tissue for dopamine and thus are robust enough to be implanted in tissue. These CNPEs are truly nanometer in dimensions and should be useful for measurements in discrete locations, including small model systems, synapses, and at living cells.

Supplementary Material

Refer to Web version on PubMed Central for supplementary material.

Acknowledgments:

This work was funded by NIH R01EB026497 (BJV and MVM) and NIHR01MH085159 (BJV) and NSF CHE-1763337 (MVM).

References:

(1). Ambrosi A; Pumera M Chem. Soc. Rev 2016, 45.

(2). Runnels PL; Joseph JD; Logman MJ; Wightman RM Anal. Chem 1999, 71 (14), 2782–2789. [PubMed: 10424168]

(3). Chen P; McCreery RL Anal. Chem 1996, 68 (22), 3958–3965.

(4). Yang C; Denno ME; Pyakurel P; Venton BJ Anal. Chim. Acta 2015, 887, 17–37. [PubMed: 26320782]

(5). Özel RE; Wallace KN; Andreescu S Anal. Chim. Acta 2011, 695 (1), 89–95. [PubMed: 21601035]

(6). Makos MA; Kim Y-C; Han K-A; Heien ML; Ewing AG Anal. Chem 2009, 81 (5), 1848–1854. [PubMed: 19192966]

(7). Shin M; Field TM; Stucky CS; Furgurson MN; Johnson MA ACS Chem. Neurosci 2017, 8 (9), 1880–1888. [PubMed: 28617576]

(8). Li Y-T; Zhang S-H; Wang L; Xiao R-R; Liu W; Zhang X-W; Zhou Z; Amatore C; Huang W-H Angew. Chem., Int. Ed 2014, 53 (46), 12456–12460.

(9). Koehne JE; Marsh M; Boakye A; Douglas B; Kim IY; Chang S-Y; Jang D-P; Bennet KE; Kimble C; Andrews R; Meyyappan M; Lee KH Analyst 2011, 136 (9), 1802–1805. [PubMed: 21387028]

(10). Strein TG; Ewing AG Anal. Chem 1992, 64 (13), 1368–1373.

(11). Shen M; Colombo ML Anal. Methods 2015, 7 (17), 7095–7105. [PubMed: 26327927]

(12). Morris CA; Friedman AK; Baker LA Analyst 2010, 135 (9), 2190–2202. [PubMed: 20563341]

(13). Clausmeyer J; Schuhmann W TrAC - Trends in Analytical Chemistry. 2016, pp 46–59.

(14). Mirkin MV; Nogala W; Velmurugan J; Wang Y Phys. Chem. Chem. Phys 2011, 13 (48), 21196–21212. [PubMed: 22031463]

(15). Rees HR; Anderson SE; Privman E; Bau HH; Venton BJ Anal. Chem 2015, 87 (7), 3849–3855. [PubMed: 25711512]

(16). Yu Y; Mirkin MV; Gao Y; Mashtalir O; Friedman G; Gogotsi Y Anal. Chem 2014, 86, 3365–3372. [PubMed: 24655227]

(17). Arrigan DWM Analyst 2004, 129 (12), 1157–1165. [PubMed: 15565213]

(18). Takahashi Y; Shevchuk AI; Novak P; Murakami Y; Shiku H; Korchev YE; Matsue TJ Am. Chem. Soc 2010, 132 (29), 10118–10126.

(19). Schrlau MG; Brailoiu E; Patel S; Gogotsi Y; Dun NJ; Bau HH Nanotechnology 2008, 19 (32), 325102. [PubMed: 21828806]

(20). Schrlau MG; Dun NJ; Bau HH ACS Nano 2009, 3 (3), 563–568. [PubMed: 19309170]

(21). Li Y; Hu K; Yu Y; Rotenberg SA; Amatore C; Mirkin MV J. Am. Chem. Soc 2017, 139 (37), 13055–13062. [PubMed: 28845981]

(22). Bucher ES; Wightman RM Annu. Rev. Anal. Chem. (Palo Alto. Calif). 2015, 8, 239–261. [PubMed: 25939038]

(23). Strand AM; Venton BJ Anal. Chem 2008, 80 (10), 3708–3715. [PubMed: 18416534]

(24). Schrlau MG; Falls EM; Ziober BL; Bau HH Nanotechnology 2008, 19 (1), 015101. [PubMed: 21730521]

(25). Hu K; Wang Y; Cai H; Mirkin MV; Gao Y; Friedman G; Gogotsi Y Anal. Chem 2014, 86 (18), 8897–8901. [PubMed: 25160727]

(26). Wilde P; Quast T; Aiyappa HB; Chen Y-T; Botz A; Tarnev T; Marquitan M; Feldhege S; Lindner A; Andronescu C; Schuhmann W ChemElectroChem 2018, 5 (20), 3083–3088.

(27). Muguruma H; Inoue Y; Inoue H; Ohsawa TJ Phys. Chem. C 2016, 120 (22), 12284–12292.

(28). Yang C; Wang Y; Jacobs CB; Ivanov I; Venton BJ Anal. Chem 2017, 5605–5611. [PubMed: 28423892]

(29). Yang C; Trikantzopoulos E; Nguyen MD; Jacobs CB; Wang Y; Mahjouri-Samani M; Ivanov IN; Venton BJ ACS Sensors 2016, 508–515. [PubMed: 27430021]

(30). Vitol EA; Schrlau MG; Bhattacharyya S; Ducheyne P; Bau HH; Friedman G; Gogotsi Y Chem. Vap. Depos 2009, 15 (7–9), 204–208.

(31). Roberts JG; Moody BP; McCarty GS; Sombers LA Langmuir 2010, 26 (11), 9116–9122. [PubMed: 20166750]

(32). Wang D; Mirkin MV J. Am. Chem. Soc 2017, 139 (34), 11654–11657. [PubMed: 28797167]

(33). Yang C; Jacobs CB; Nguyen MD; Ganesana M; Zestos AG; Ivanov IN; Puretzky AA; Rouleau CM; Geohegan DB; Venton BJ Anal. Chem 2016, 88, 645–652. [PubMed: 26639609]

(34). Yang C; Trikantzopoulos E; Jacobs CB; Venton BJ Anal. Chim. Acta 2017, 965, 1–8. [PubMed: 28366206]

(35). Takmakov P; Zachek MK; Keithley RB; Walsh PL; Donley C; McCarty GS; Wightman RM Anal. Chem 2010, 82 (5), 2020–2028. [PubMed: 20146453]

(36). Xiao N; Privman E; Venton BJ ACS Chem. Neurosci 2014, 5 (8), 666–673. [PubMed: 24849718]

(37). Ping J; Wu J; Wang Y; Ying Y Biosens. Bioelectron 2012, 34 (1), 70–76. [PubMed: 22341755]

(38). Chen C-H; Luo S-C ACS Appl. Mater. Interfaces 2015, 7, 21931–21938. [PubMed: 26381224]

(39). Hočevar SB; Wang J; Deo RP; Musameh M; Ogorevc B Electroanalysis 2005, 17 (5–6), 417–422.

(40). Peairs MJ; Ross AE; Venton BJ Anal. Methods 2011, 3 (10), 2379–2386.

(41). Zestos AG; Yang C; Jacobs CB; Hensley D; Venton BJ Analyst 2015, 140, 7283–7292. [PubMed: 26389138]

(42). Roberts JG; Toups JV; Eyualem E; McCarty GS; Sombers LA Anal. Chem 2013, 85 (23), 11568–11575. [PubMed: 24224460]

(43). Ruiz JJ; Rodriguez-mellado JM; Dominguez M; Aldaz AJ Chem. Soc. Faraday Trans 1989, 85 (7), 1567–1574.

(44). Trikantzopoulos E; Yang C; Ganesana M; Wang Y; Venton BJ Analyst 2016, 141 (18), 5256–5260. [PubMed: 27536741]

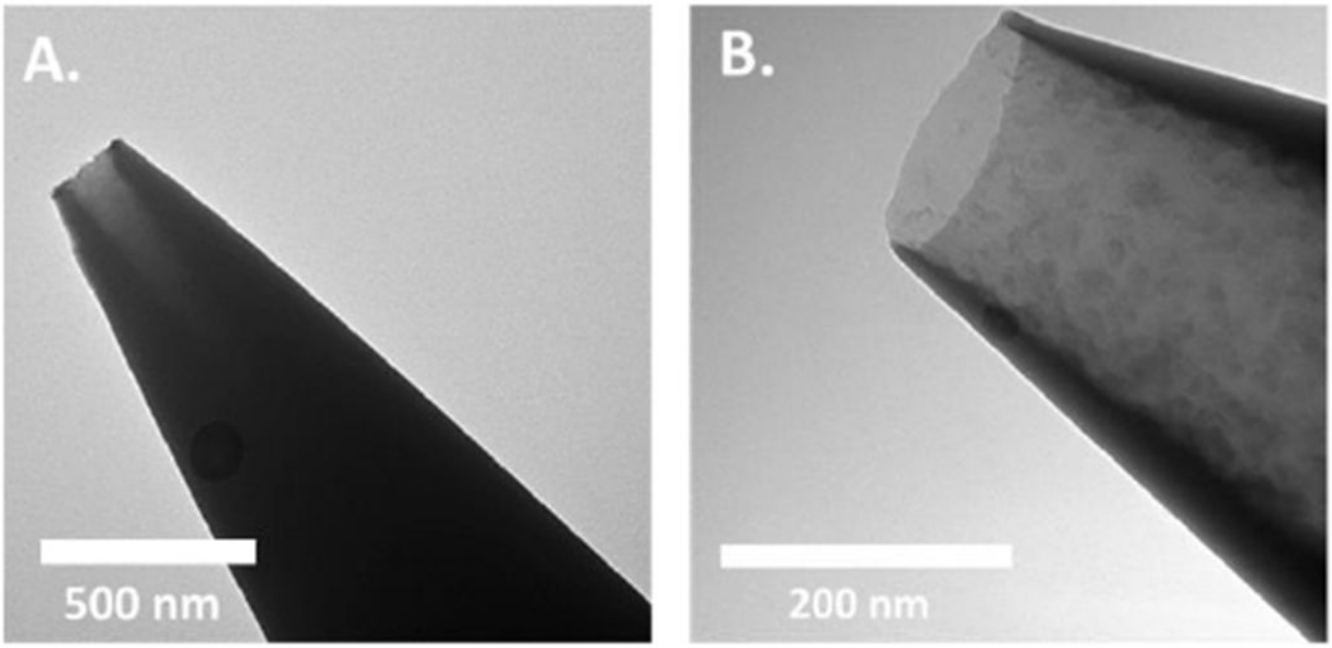

Figure 1.

TEM image of (A) a cavity carbon nanopipette electrodes with the cavity depth of about 500 nm and the orifice diameter of about 200 nm, and (B) an open-tube CNPE with the orifice diameter of about 200 nm and a long depth.

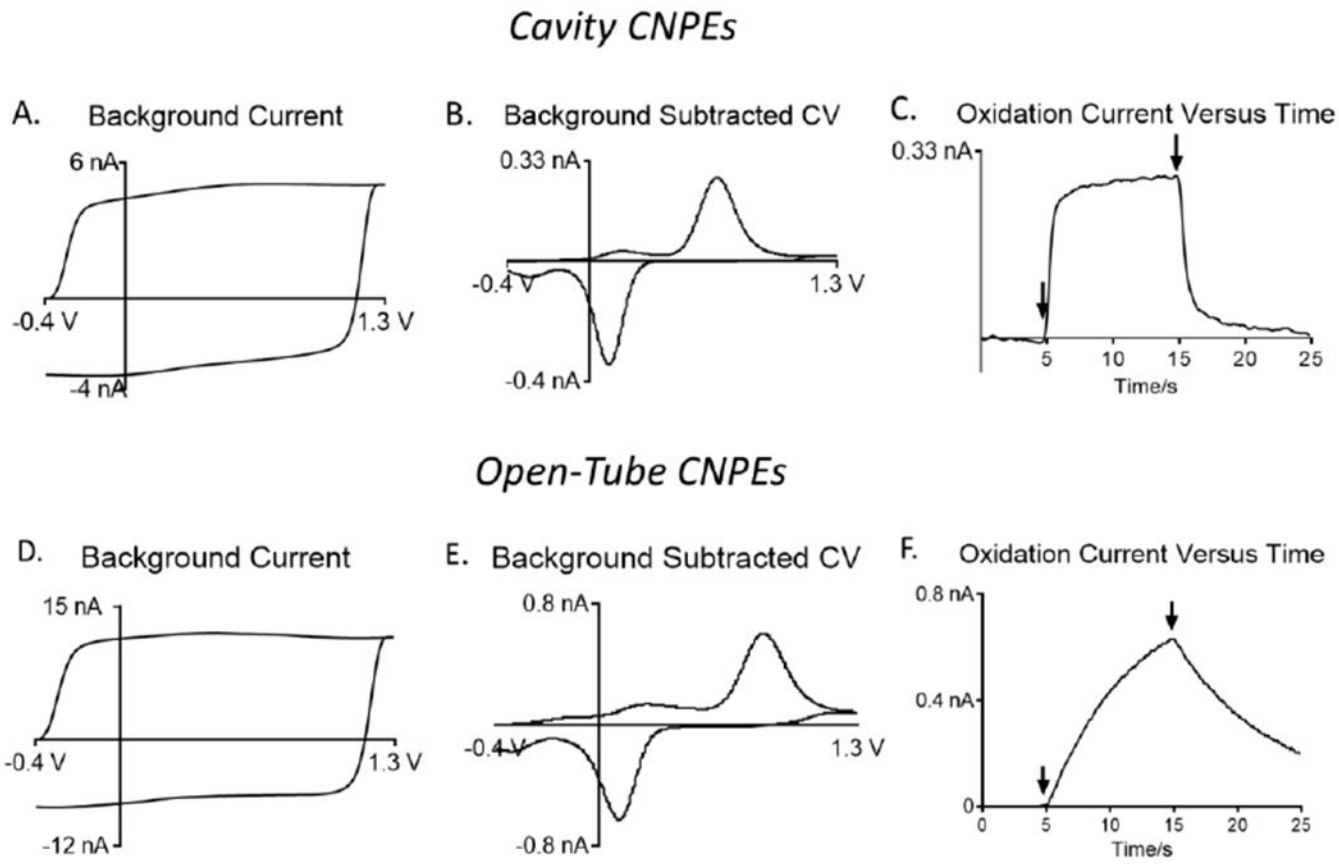

Figure 2.

Electrochemical response to 5 μM dopamine at a cavity CNPE (A-C) and an open tube CNPE (D-F). Measurements were obtained at scan rate of 400 V/s and scan repetition frequency of 10 Hz. (A, D) Background currents in PBS buffer, (B, E) background subtracted cyclic voltammogram to 5 μM dopamine, and (C, F) measured oxidation current versus time for a flow injection analysis experiment (dopamine bolus injection and changing back to PBS buffer are marked as black arrows).

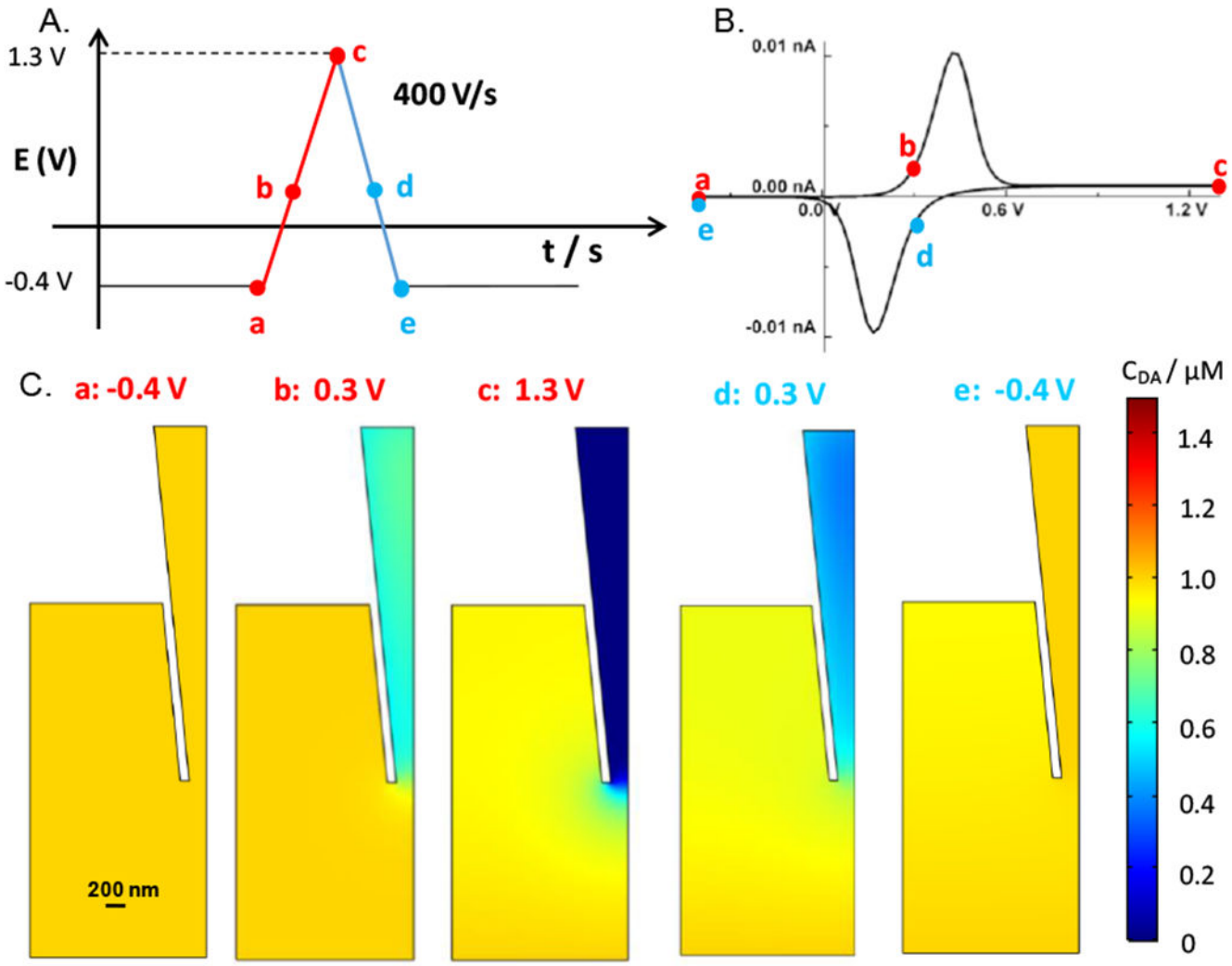

Figure 3.

Numerical simulation of the dopamine oxidation/reduction with cavity CNPEs. (A) FSCV waveform showing potentials where concentrations were modeled. (B) Modeled cyclic voltammogram for dopamine. Symmetric peaks show the thin layer cell effects. (C) Modeled concentrations of dopamine inside the pipette. The rectangle is the reservoir of 1 µM dopamine. Half of a nanopipette is shown. On the anodic ramp, at 0.3 V, dopamine starts to be oxidized and by 1.3 V, there is complete oxidation of all DA in the CNPE. On the cathodic ramp, dopamine is being reformed by reduction at 0.3 V and by −0.4 V all of the dopamine has been redox recycled back from dopamine-o-quinone. For all simulations, the scan rate is 400 V/s, σ = −0.01 C/m^2, radius=200 nM, H = 20.

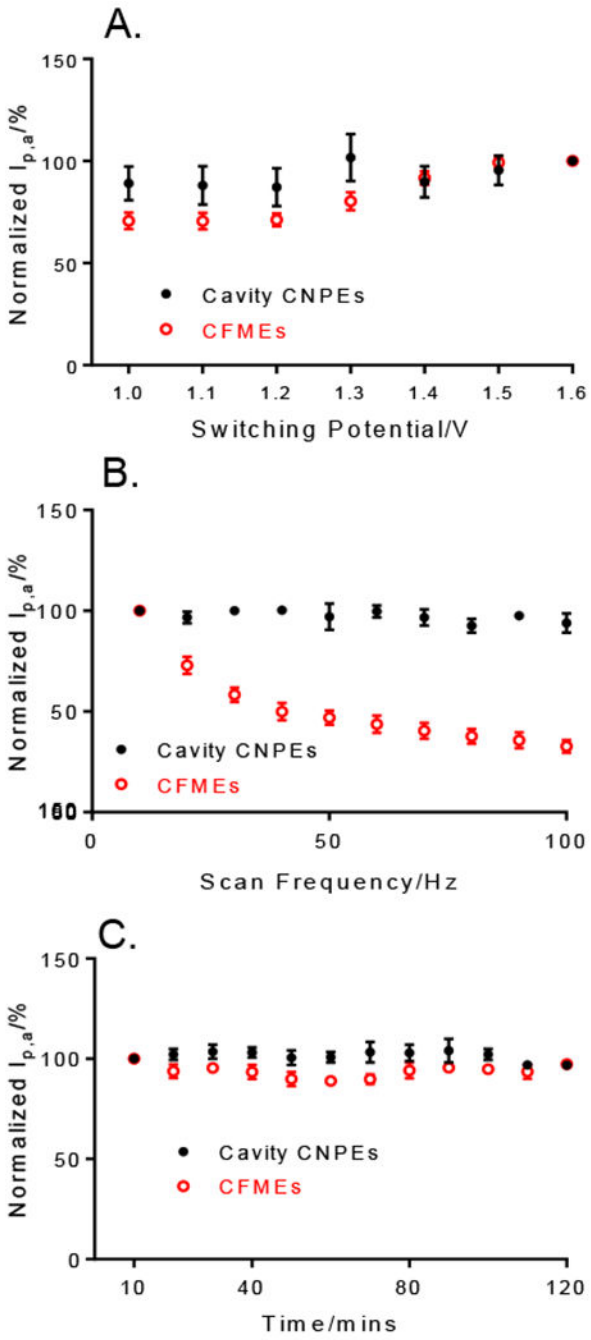

Figure 4.

(A) Effect of switching potential. The plot shows average oxidation current for 1 μM dopamine at cavity CNPEs (black dot, n = 5) and CFMEs (red circle, n = 5) for each switching potential (1.0 V to 1.6 V, with the interval of 0.1 V) with a triangle waveform from −0.4 V and 400 V/s scan rate. Peak currents were normalized to the current using the 1.6 V waveform. (B) Effect of scan repetition frequency. Peak oxidation current at cavity CNPEs (black dot, n = 4) and CFMEs (red circle, n = 5) with −0.4 to 1.3 V waveform and scan rate of 400 V/s. Peak currents were normalized to the current at 10 Hz. (C) Two-hour

stability test of cavity CNPEs with constant waveform application (−0.4 to 1.3V, 400 V/s, 10 Hz) (black dot, n = 3) compared to CFMEs (red circle, n = 3). Oxidation current to 1 μM dopamine was normalized to the signal observed after 10 minutes equilibration. Error bars are the standard error of the mean.

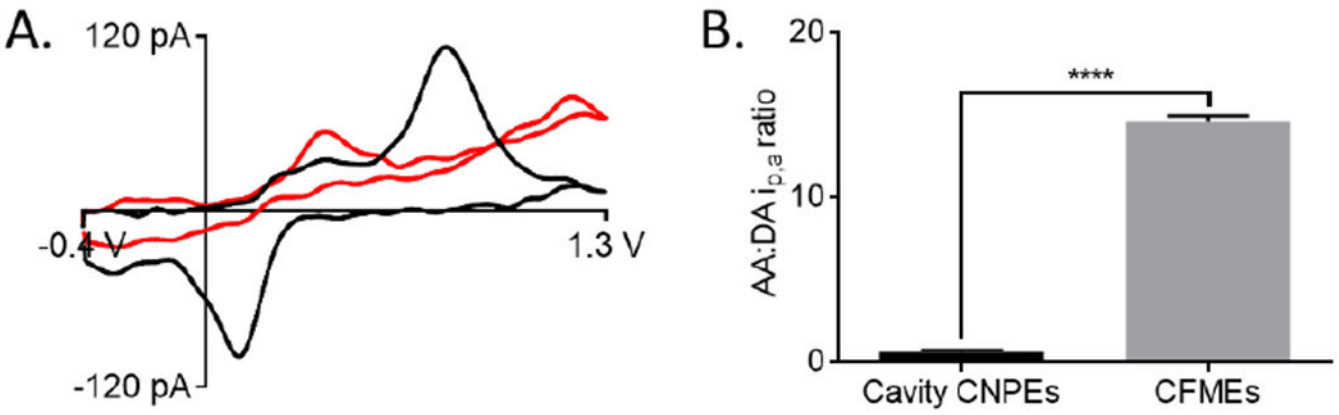

Figure 5.

(A) CVs of 200 μM ascorbic acid (red line) and 1 μM dopamine obtained from the same cavity CNPE and CFME. (B) Column plots show the ratio of oxidation current for 200 μM ascorbic acid compared to the corresponding oxidation current of dopamine at cavity CNPEs (black, n = 5) and CFMEs (gray, n = 5). The oxidation current ratio at cavity CNPEs is significantly smaller than CFMEs for the measurement of ascorbic acid (t test,$p \leq 0.0001$).

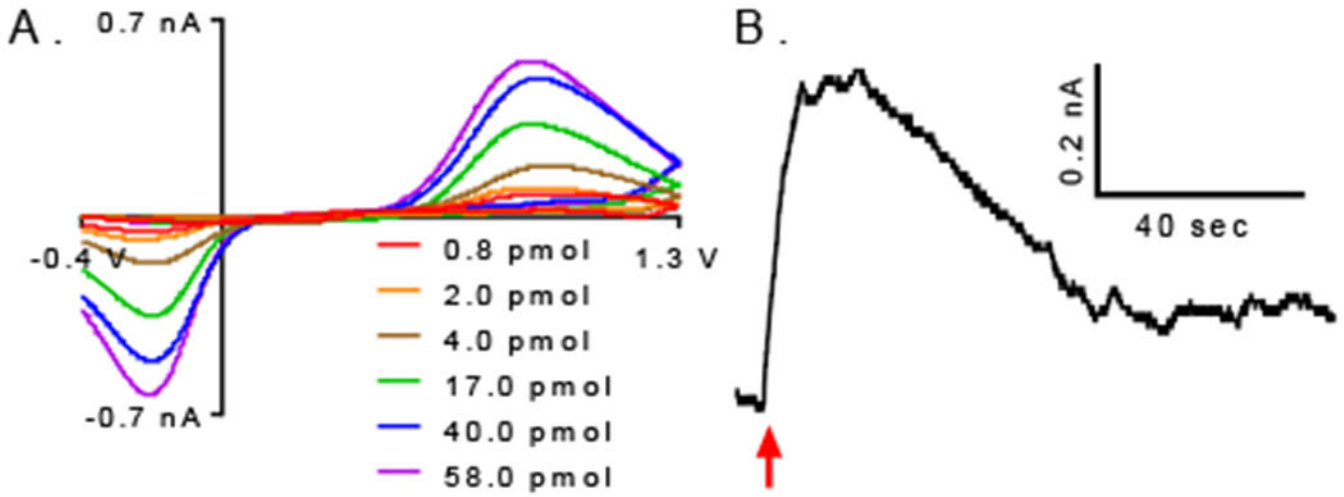

Figure 6.

Electrochemical response of cavity CNPEs to exogenous dopamine application. Measurements were obtained at a scan rate of 400V/s and at a scan rate frequency of 10 Hz. (A) Background subtracted CVs of the same electrode with varying the time for dopamine application (pressure kept constant). The pressure-ejection times (0.02 to 1.5 seconds) were converted to molar quantities released by the picospritzing pipette using the initial concentration of the dopamine solution (150 μM) and the volume of solution released for each duration. (B) The oxidative current versus time for a different electrode with a 1 second puff of dopamine (27.0 pmol). The dopamine was ejected at the arrow.

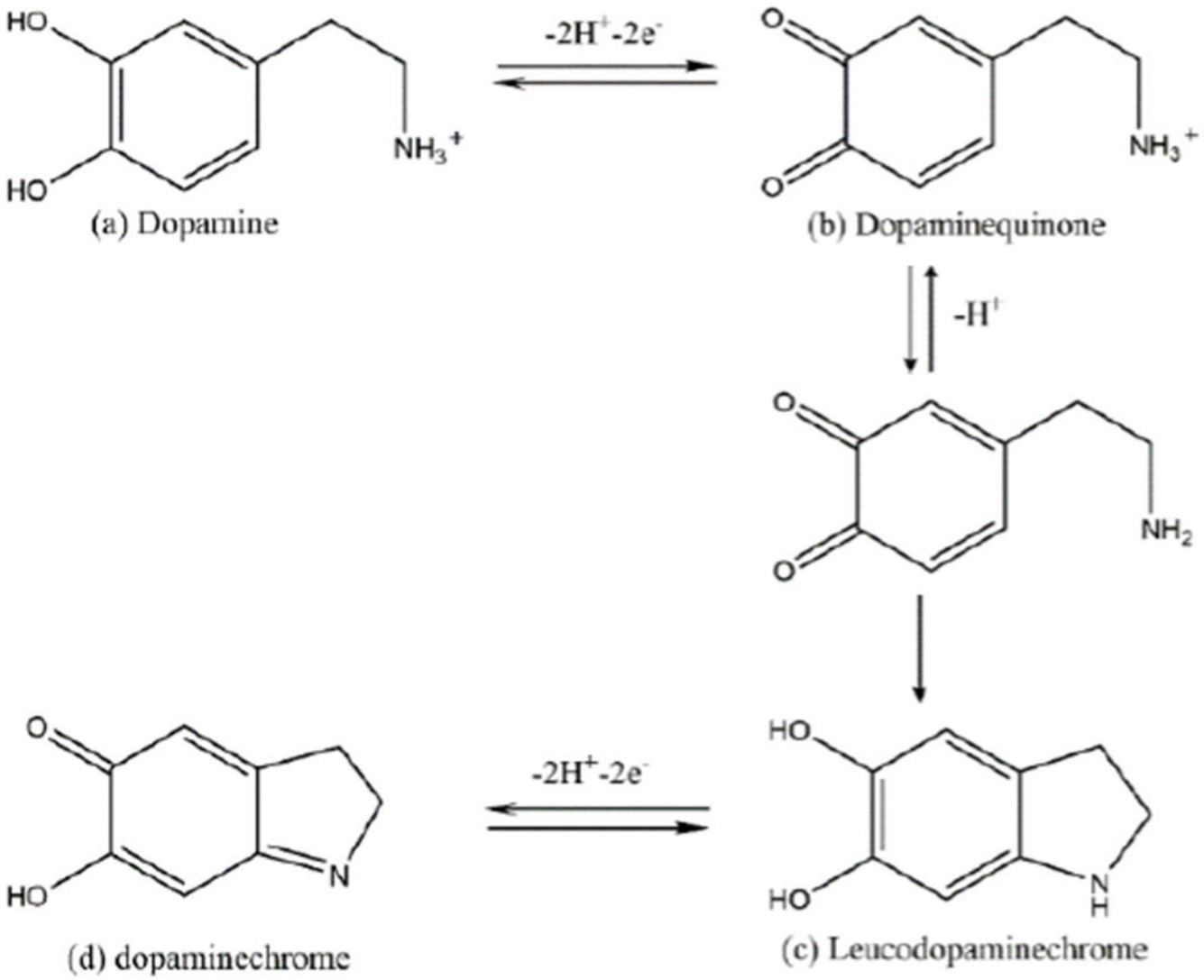

Scheme 1.
Dopamine oxidation scheme.

Table 1.

Comparison of Dopamine Detection at Cavity CNPEs, Conical CNPEs, and CFMEs[a]

	i_{BG} (nA)	$i_{p,a}$ (nA)	$i_{p,a}/i_{BG}$ ratio	LOD (nM)	ΔE_p (V)	$i_{p,a}/i_{p,c}$
Cavity CNPE n = 5	5.7 ± 0.5	0.19 ± 0.02	0.0326 ± 0.004	56 ± 13	0.62 ± 0.03	1.18 ± 0.09
Conical CNPE[15] n= 8	410 ± 80 ****	14 ± 3 ****	0.0246 ± 0.009 ***	25 ± 5 *	0.52 ± 0.01 *	1.40±0.10 ***
CFME n= 6	570 ± 160 ****	19 ± 2 ****	0.0463± 0.010 ****	19 ± 4 **	0.67 ± 0.01 **	1.59 ± 0.03 ****

[a] All values for 1 μM dopamine detection.

Electrochemical measurements were performed with a FSCV waveform scanning from −0.4 to 1.3 V and back at 400 V/s, with scan repetition frequency of 10 Hz. Significantly different than cavity CNPEs:

**** unpaired t test, $p \leq 0.0001$,

*** unpaired t test, $p \leq 0.001$,

** unpaired t test, $p \leq 0.01$,

* unpaired t test, $p \leq 0.05$.